Article

Optimal Terminations for a Single-Input Multiple-Output Resonant Inductive WPT Link

Giuseppina Monti [1,*,†], Mauro Mongiardo [2,†], Ben Minnaert [3] , Alessandra Costanzo [4] and Luciano Tarricone [1]

[1] Department of Engineering for Innovation, University of Salento, 73100 Lecce, Italy; luciano.tarricone@unisalento.it
[2] Department of Engineering, University of Perugia, 06123 Perugia, Italy; mauro.mongiardo@unipg.it
[3] Department of Industrial Science and Technology, Odisee University College of Applied Sciences, 9000 Ghent, Belgium; ben.minnaert@odisee.be
[4] Department of Electrical, Electronic and Information Engineering Guglielmo Marconi, University of Bologna, 40126 Bologna, Italy; alessandra.costanzo@unibo.it
* Correspondence: giuseppina.monti@unisalento.it
† These authors contributed equally to this work.

check for updates

Abstract: This paper analyzes a resonant inductive wireless power transfer link using a single transmitter and multiple receivers. The link is described as an $(N+1)$–port network and the problem of efficiency maximization is formulated as a generalized eigenvalue problem. It is shown that the desired solution can be derived through simple algebraic operations on the impedance matrix of the link. The analytical expressions of the loads and the generator impedances that maximize the efficiency are derived and discussed. It is demonstrated that the maximum realizable efficiency of the link does not depend on the coupling among the receivers that can be always compensated. Circuital simulation results validating the presented theory are reported and discussed.

Keywords: resonant; wireless power transfer; inductive coupling; optimal load; single-input multiple-output; power gain

1. Introduction

In recent years, several applications have been proposed for resonant inductive Wireless Power Transfer (WPT) [1–4]. In fact, resonant inductive WPT is an effective solution for wirelessly energizing electronic devices and several optimal design strategies have been investigated in the literature.

Usually, the goal is to recharge a single device and the focus is on maximizing either the power delivered to the load or the power transfer efficiency. In this regard, the most widely adopted scheme is that using a single transmitter, thus corresponding to a Single-Input Single Output (SISO) configuration. In a SISO configuration the link consists of just two magnetically coupled resonators: a transmitting resonator connected to the source and a receiving resonator connected to the load (i.e., the device to be recharged). SISO configurations have been widely investigated in the literature and it has been demonstrated that the link has to be terminated on its conjugate image impedances for maximizing both the power on the loads and the efficiency [5–7].

More recently, schemes using multiple transmitters and/or multiple receivers have been also investigated. The use of Multiple Input Single Output (MISO) schemes could be adopted to obtain an almost constant performance on a given area/volume this being useful if the position of the receiver is affected by small uncertainties (as in the case of embedded devices). In this regard, some interesting results are reported in [8] where it is demonstrated that a two-dimensional region of nearly constant

power transfer efficiency can be obtained by using four transmitters. In [9] the use of a linear array of transmitters, activated two at time, is suggested for providing a constant output voltage to a load moving along a linear path. The problem of maximizing the efficiency and the power on the load in MISO schemes has been also analyzed and some interesting results have been reported in [10,11]. In particular, in [10] the solution for maximizing the efficiency has been formulated as a convex optimization problem. In [11] the optimal loads for both the maximum power and the maximum efficiency solutions have been presented for the case of a link using either two–transmitter and a single load or a single transmitter and two–load. In [12], a more abstract approach was used to maximize the efficiency by modeling the MISO-WPT system as a linear circuit whose input-output relationship is expressed in terms of a small number of unknown parameters that can be thought of as transimpedances and gains.

As per schemes using a Single Transmitter and Multiple Receivers (SIMO), they are adopted to recharge multiple devices with a single transmitter [13–28]. In [20] the use of a multiple-output scheme is suggested for the recharge of electric vehicles. The problem of maximizing the power delivered to the loads has been solved in [21], where the expressions of the optimal loads have been derived by using the maximum power transfer theorem for an *N*–port.

As per the problem of efficiency maximization, in [23] the use of suitable matching networks is suggested. In [24], the specific case of a link using two receivers is analyzed and it is demonstrated that for some specific configurations of the receivers it is convenient to use a non-synchronous scheme with receivers resonating at a frequency different from that of the transmitter. In [22] a SIMO system with constant output voltage and operating at 6.78 MHz is presented. The efficiency of the proposed WPT link is optimized by tuning the input voltage at the transmitter side.

In [25], the loads for maximizing the efficiency have been derived from the expression calculated for the case of a link using one receiver and that using two receivers. However, the analysis is performed assuming that the coupling among the receivers can be neglected, this representing a limitation for real applications. The presence of possible couplings among the receivers has been analyzed in [26,27]. It is demonstrated that for given loads a coupling among the receivers can be compensated by using suitable compensating reactances; however, in these papers it is assumed that the loads are given (i.e., they are not optimized).

Finally, for the problem of efficiency maximization, elegant and comprehensive analysis of all possible configurations (i.e., the SIMO, MISO and MIMO configurations) have been presented in [29,30]. A very elegant and general approach is presented in [29]; where, starting from the impedance or scattering matrix of a multiport the efficiency of a generic MIMO-WPT system is expressed by the Rayleigh quotient. However, the method is not applied on an inductive WPT system and the optimal loads are only expressed as function of the port currents and impedance matrix elements. In [30], the optimal loads are derived from the first-order necessary condition consisting of imposing the zeroing of the first-order partial derivatives of the efficiency with respect to the input and output currents. The optimal solution derived in this way is validated by checking the second order derivatives. The developed analysis is general and overcomes some limitations present in the previous literature. For instance, for the SIMO case a generic number of possibly coupled receivers is considered. Similarly, for the MISO case, the formulas are presented for a generic number of possibly coupled transmitters. However, the analysis developed in [30] is based on the assumption that all the couplings among the transmitters and the receivers are purely inductive; this assumption limits the applicability of the approach to practical applications where the conductivity of the propagation channel is negligibly small.

In this paper, referring to the SIMO configuration, similarly to [29], the problem of finding the optimal loads maximizing the efficiency is formulated as a generalized eigenvalue problem. The presented theory is valid for any strictly passive and reciprocal network in SIMO configuration and is applied in detail for the first time in this paper to the case of a resonant inductive WPT link. The application of the presented theory just requires the knowledge of the impedance matrix of

the SIMO network that can be the result of measurements, simulations or theoretical derivation. The network must not satisfy any particular hypothesis except that of being passive and reciprocal; consequently, the proposed approach is also applicable in the case of non-purely inductive couplings (including the case of a propagation channel with non-negligible values of the conductivity).

The general theory is first presented for a generic $(N + 1)$–port network in SIMO configuration and then applied to the specific case of a resonant inductive WPT link; the analytical expressions of the complex loads maximizing the efficiency are derived and discussed. Additionally, the importance of suitably selecting the generator impedance for maximizing the total output power corresponding to the maximum efficiency solution is discussed. The correctness of the derived expressions is validated by the results reported in [30] and by numerical data presented in this paper.

The paper is organized as follows. In Section 2 the problem of efficiency maximization is solved for a generic SIMO $(N + 1)$–port network. In Section 3 the derived equations are specialized for the case of an inductive WPT link, the optimal expressions of the loads and the generator impedances are reported. In Section 4 theoretical formulas are validated through circuital and full-wave simulations. Finally, some conclusions are drawn in Section 5.

2. Derivation of the Solution for the General Case

The problem analyzed in this paper is a WPT link using a Single-Input Multiple-Output (SIMO) configuration: a single transmitter is wirelessly connected to N receivers. In this section, the general case is analyzed, no specific assumption is made on the coupling mechanism among the transmitter and the receivers, it is only assumed that the network is passive and reciprocal.

By using a network formalism, the link is modeled as an $(N + 1)$–port network $\mathfrak{N}$, see Figure 1, described by its impedance matrix $\mathbf{Z}$. The input port is connected to a sinusoidal source V_G with internal impedance Z_G and the output ports are connected to an N-port load $\mathfrak{N}_L$ with impedance matrix $\mathbf{Z}_L$. Generally, in practical cases, $\mathfrak{N}_L$ consists of a set of N uncoupled load impedances and, consequently, $\mathbf{Z}_L$ is a diagonal matrix

$$\mathbf{Z}_L = \mathrm{diag}(Z_{L,n}), \tag{1}$$

with $n = 1, \ldots, N$.

In real applications, the generator could be a complex network, comprising a DC-AC converter and other circuitry. Accordingly, in general, Z_G is the input impedance of the network adopted for generating the power to be provided at the input port of the network $\mathfrak{N}$. The same consideration applies for each load. In fact, in real applications each load can be a more or less complicated network which in most cases includes a rectifier for converting the AC power at the output port of the network into a DC signal. Accordingly, the generic impedance Z_{Li} is the input impedance of the network connected to the output port i of the link.

The vectors of voltage and current phasors at the network ports, $\mathbf{V}$ and $\mathbf{I}$, and the matrix $\mathbf{Z}$ can be partitioned as

$$\left[\begin{array}{c} V_\mathrm{i} \\ \hline \mathbf{V}_\mathrm{o} \end{array} \right] = \left[\begin{array}{c|c} Z_\mathrm{ii} & \mathbf{Z}_\mathrm{io} \\ \hline \mathbf{Z}_\mathrm{oi} & \mathbf{Z}_\mathrm{oo} \end{array} \right] \left[\begin{array}{c} I_\mathrm{i} \\ \hline \mathbf{I}_\mathrm{o} \end{array} \right] \tag{2}$$

where V_i and I_i represent voltage and current at the input port, while $\mathbf{V}_\mathrm{o}$ and $\mathbf{I}_\mathrm{o}$ are the N-vectors of voltages and currents at the output ports.

By replacing the load equation

$$\mathbf{V}_\mathrm{o} = -\mathbf{Z}_\mathrm{L} \mathbf{I}_\mathrm{o} \tag{3}$$

in (2), and by eliminating $\mathbf{I}_\mathrm{o}$, the impedance seen at the input port of $\mathfrak{N}$ can be derived as

$$Z_\mathrm{in} = \frac{V_\mathrm{i}}{I_\mathrm{i}} = Z_\mathrm{ii} - \mathbf{Z}_\mathrm{io} \left(\mathbf{Z}_\mathrm{oo} + \mathbf{Z}_\mathrm{L} \right)^{-1} \mathbf{Z}_\mathrm{oi}. \tag{4}$$

In a similar way, by combining (2) with the source equation

$$V_i = V_G - Z_G I_i \tag{5}$$

and eliminating I_i, the relation between voltages and currents at the output ports can be cast in the form

$$\mathbf{V}_o = \mathbf{V}_{th} + \mathbf{Z}_{out} \mathbf{I}_o \tag{6}$$

where

$$\mathbf{V}_{th} = \frac{\mathbf{Z}_{oi} V_G}{Z_{ii} + Z_G} \tag{7}$$

is a set of N Thévenin equivalent voltage sources and

$$\mathbf{Z}_{out} = \mathbf{Z}_{oo} - \frac{\mathbf{Z}_{oi} \mathbf{Z}_{io}}{Z_{ii} + Z_G} \tag{8}$$

is the equivalent impedance matrix of the network $\mathfrak{N}$ with the input port closed on the impedance Z_G. The network $\mathfrak{N}$ can be thus represented by the equivalent circuit of Figure 2.

The maximum power transfer between the source and the input port of $\mathfrak{N}$ can be achieved when the conjugate match condition

$$Z_G = Z_{in}^*, \tag{9}$$

where * denotes conjugation, is satisfied. In this case, the power delivered to $\mathfrak{N}$ is equal to the generator available power

$$P_{AG} = \frac{|V_G|^2}{8 \operatorname{Re}[Z_G]}. \tag{10}$$

As far as the output side is concerned, it can be proved [31] that the power delivered by $\mathfrak{N}$ is maximized when the output currents $\mathbf{I}_o$ assume the values $\mathbf{I}_{oM}$ given by

$$\mathbf{I}_{oM} = - \left(\mathbf{Z}_{out} + \mathbf{Z}_{out}^\dagger \right)^{-1} \mathbf{V}_{th} \tag{11}$$

where † denotes conjugate transpose, and consequently the available power at the output ports of $\mathfrak{N}$ is

$$P_a = \frac{1}{4} \mathbf{V}_{th}^\dagger \left(\mathbf{Z}_{out} + \mathbf{Z}_{out}^\dagger \right)^{-1} \mathbf{V}_{th}. \tag{12}$$

It can be noted that for $N > 1$, the optimal load is not univocally defined. In fact, the optimal currents can be obtained by any impedance matrix $\mathbf{Z}_{Lm}$ such that

$$\mathbf{Z}_{LM} \mathbf{I}_{oM} = \mathbf{Z}_{out}^\dagger \mathbf{I}_{oM} = -\mathbf{V}_{oM} \tag{13}$$

where $\mathbf{V}_{oM}$ are the voltages at output ports for $\mathbf{I}_o = \mathbf{I}_{oM}$. Equation (13) also shows that it is possible to realize $\mathbf{Z}_{LM}$ as a set of N independent passive impedances provided that the possible zero elements of $\mathbf{I}_{oM}$ corresponds to zero elements of $\mathbf{V}_{oM}$, and that the phase difference between any two corresponding elements of $\mathbf{I}_{oM}$ and $\mathbf{V}_{oM}$ is $\geq 90°$ in absolute value.

According to the previous discussion, also the problem of determining the impedances Z_G and $\mathbf{Z}_L$ which provide the simultaneous maximum power transfer at the input and output ports has not a unique solution.

To simplify the calculation of the optimal terminations, it is convenient to determine the corresponding optimal currents, which, on the contrary, are univocally defined.

Making use of (2), the total power delivered to the loads P_o, i.e., the sum of the powers delivered to each load P_{oi}

$$P_\text{o} = \sum_{n=1}^{N} P_{oi},$$ (14)

can be expressed as a function of the port currents as

$$
\begin{aligned}
P_\text{o} &= -\frac{1}{4} \left(\mathbf{V}_\text{o}^\dagger \mathbf{I}_\text{o} + \mathbf{I}_\text{o}^\dagger \mathbf{V}_\text{o} \right) = \\
&= -\frac{1}{4} \left[\mathbf{I}_\text{o}^\dagger \left(\mathbf{Z}_\text{oo} + \mathbf{Z}_\text{oo}^\dagger \right) \mathbf{I}_\text{o} + \mathbf{I}_\text{o}^\dagger \mathbf{Z}_\text{oi} I_\text{i} + I_\text{i}^* \mathbf{Z}_\text{oi}^\dagger \mathbf{I}_\text{o} \right]
\end{aligned}
$$ (15)

and, similarly, the input power can be expressed as

$$
\begin{aligned}
P_\text{i} &= \frac{1}{4} \left(V_\text{i}^* I_\text{i} + I_\text{i}^* V_\text{i} \right) = \\
&= \frac{1}{4} \left[I_\text{i}^* \left(Z_\text{ii} + Z_\text{ii}^* \right) I_\text{i} + I_\text{i}^* \mathbf{Z}_\text{io} \mathbf{I}_\text{o} + \mathbf{I}_\text{o}^\dagger \mathbf{Z}_\text{io}^\dagger I_\text{i} \right].
\end{aligned}
$$ (16)

The previous equations can be cast in the form

$$
\begin{aligned}
P_\text{o} &= \frac{1}{4} \mathbf{I}^\dagger \mathbf{A} \mathbf{I} \\
P_\text{i} &= \frac{1}{4} \mathbf{I}^\dagger \mathbf{B} \mathbf{I}
\end{aligned}
$$ (17)

where the matrices $\mathbf{A}$ and $\mathbf{B}$ are defined as

$$
\mathbf{A} = - \left[\begin{array}{c|c} 0 & \mathbf{Z}_\text{oi}^\dagger \\ \hline \mathbf{Z}_\text{oi} & \mathbf{Z}_\text{oo} + \mathbf{Z}_\text{oo}^\dagger \end{array} \right]
$$ (18)

$$
\mathbf{B} = \left[\begin{array}{c|c} Z_\text{ii} + Z_\text{ii}^* & \mathbf{Z}_\text{io} \\ \hline \mathbf{Z}_\text{io}^\dagger & 0 \end{array} \right].
$$ (19)

The power gain of $\mathfrak{N}$, defined as the ratio between the output and the input power, can thus be expressed as

$$
G_\text{P} = \frac{P_\text{o}}{P_\text{i}} = \frac{\mathbf{I}^\dagger \mathbf{A} \mathbf{I}}{\mathbf{I}^\dagger \mathbf{B} \mathbf{I}}.
$$ (20)

In the context of WPT the quantity expressed in (20) is usually referred to as the efficiency of the link, in this paper it will be referred to as G_p in analogy with the terminology adopted in the context of two-port networks.

The power gain is maximized when the maximum power transfer is realized at the output port. Since G_P is a generalized Rayleigh quotient, the maximum of G_P can be determined by solving a generalized eigenvalue problem.

As a matter of fact, using the quotient rule and taking into account the fact that $\mathbf{A}$ and $\mathbf{B}$ are Hermitian matrices, the differential of G_P can be calculated as

$$
\delta G_\text{p} = 2 \frac{(\delta \mathbf{I}^\dagger \mathbf{A} \mathbf{I})(\mathbf{I}^\dagger \mathbf{B} \mathbf{I}) - (\mathbf{I}^\dagger \mathbf{A} \mathbf{I})(\delta \mathbf{I}^\dagger \mathbf{B} \mathbf{I})}{(\mathbf{I}^\dagger \mathbf{B} \mathbf{I})^2}.
$$ (21)

Hence, requiring $\delta G_\text{p} = 0$ yields

$$
\mathbf{A} \mathbf{I} - \frac{\mathbf{I}^\dagger \mathbf{A} \mathbf{I}}{\mathbf{I}^\dagger \mathbf{B} \mathbf{I}} \mathbf{B} \mathbf{I} = 0,
$$ (22)

which can be rewritten as

$$\mathbf{Ax} = \lambda \mathbf{Bx} \tag{23}$$

and can be recognized as a generalized eigenvalue problem with $\lambda = G_p$ being the eigenvalue and $\mathbf{x} = \mathbf{I}$ the corresponding eigenvector.

Since, by hypothesis, $\mathfrak{N}$ is passive and the power supply is provided only at the input port, the maximum power gain, G_M, and the corresponding currents (up to an arbitrary factor) can be determined by solving (23) with the constrains

$$\begin{aligned} \lambda &\leq 1 \\ P_i &\geq 0 \\ P_o &\geq 0. \end{aligned} \tag{24}$$

After determining the optimal currents

$$\mathbf{I}_M = \begin{bmatrix} I_{iM} \\ \mathbf{I}_{oM} \end{bmatrix} \tag{25}$$

by (23), the corresponding voltages

$$\mathbf{V}_M = \begin{bmatrix} V_{iM} \\ \mathbf{V}_{oM} \end{bmatrix} \tag{26}$$

can be obtained by (2). Hence the source impedance providing maximum power transfer at the input port can be calculated by letting

$$Z_{GM} = \frac{V_{iM}^*}{I_{iM}^*}, \tag{27}$$

while the maximum power transfer at the output port is obtained with any load $\mathfrak{N}_L$ whose impedance matrix satisfies (13). In particular, if the previously enunciated conditions are satisfied, $\mathfrak{N}_L$ can be realized as a set of uncoupled loads with impedances

$$Z_{LM,n} = -\frac{V_{oM,n}}{I_{oM,n}} \tag{28}$$

with $n = 1, \ldots, N$.

It is worth observing that the theory presented in this section is completely general, it can be applied to any passive SIMO network; moreover, for its application it is sufficient to know the impedance matrix of the network. It is possible to derive the maximum achievable power gain and the optimal loads starting from the impedance matrix, which can be the results of measurements, theoretical calculation or a numerical analysis. Figure 3 summarizes how to apply the proposed approach for the determination of the load impedances maximizing the efficiency of a SIMO Resonant Inductive WPT Link.
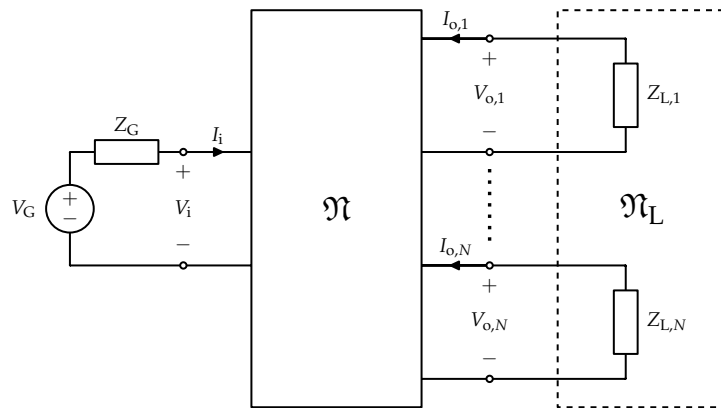
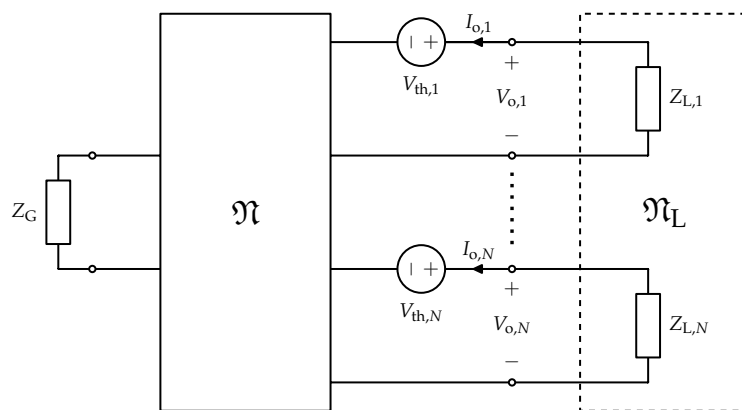**Figure 1.** Schematic representation of a SIMO WPT link.

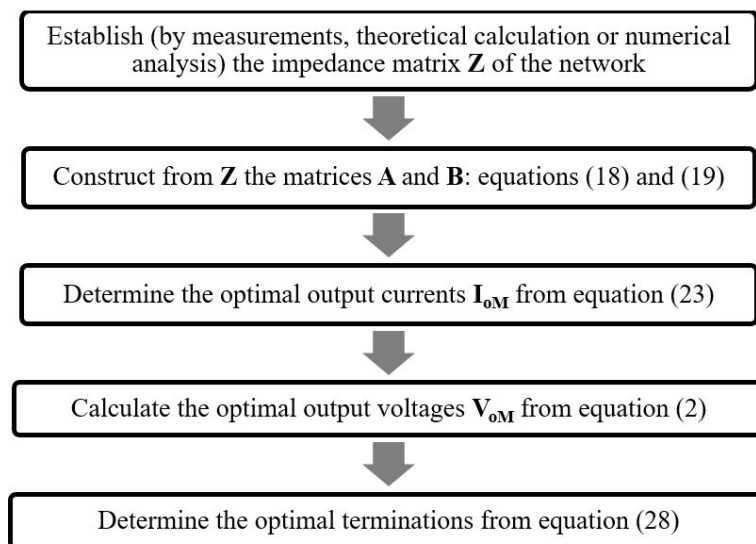**Figure 2.** Equivalent Thévenin representation of the circuit of Figure 1.

Figure 3. Block diagram of the proposed approach to determine the optimal terminations for efficiency maximization of a SIMO Resonant Inductive WPT Link.

3. The Case of an Inductive Resonant Coupling

In this section, the specific case of a WPT link consisting of $(N + 1)$ magnetically coupled resonators is considered (Figure 4). More specifically, the link consists of $(N + 1)$ magnetically coupled inductors, L_i, each one loaded by a suitable compensating capacitor, C_i, realizing the resonance

condition at the operating angular frequency (i.e., $\omega_0 = 1/\sqrt{L_i C_i}$). The inductor losses are modeled by series resistors R_i related to the quality factors of the coupled resonators:

$$Q_n = \frac{\omega L_n}{R_n}. \tag{29}$$

The coupling between the inductors L_m and L_n is described by the coupling factor k_{mn} related to the mutual inductance M_{mn}

$$k_{mn} = \frac{M_{mn}}{\sqrt{L_m L_n}}. \tag{30}$$
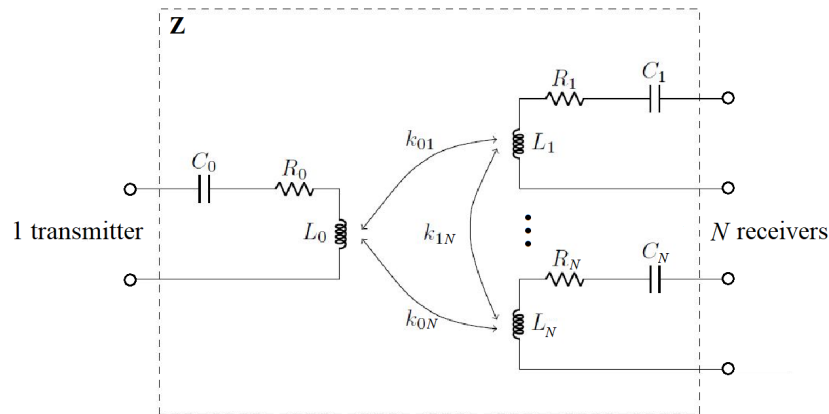

Figure 4. Equivalent circuit of a WPT link with a single transmitter and N receivers, determined by its impedance matrix $\mathbf{Z}$.

Accordingly, the network is described by the following impedance matrix:

$$\mathbf{Z} = \begin{bmatrix} R_0 & j\omega M_{01} & j\omega M_{02} & \cdots & j\omega M_{0N} \\ j\omega M_{01} & R_1 & j\omega M_{12} & \cdots & j\omega M_{1N} \\ j\omega M_{02} & j\omega M_{12} & R_2 & \cdots & j\omega M_{2N} \\ \vdots & \vdots & \vdots & \ddots & \vdots \\ j\omega M_{0N} & j\omega M_{1N} & j\omega M_{2N} & \cdots & R_N \end{bmatrix}. \tag{31}$$

By introducing the normalization matrix $\mathbf{d}$:

$$\mathbf{d} = \operatorname{diag}\left(\frac{1}{\sqrt{\omega L_n}}\right), n = 0, \ldots, N, \tag{32}$$

it is possible to obtain the following normalized expression for the impedance matrix of the network:

$$\mathbf{z} = \mathbf{dZd} = \begin{bmatrix} \dfrac{1}{Q_0} & jk_{01} & jk_{02} & \cdots & jk_{0N} \\ jk_{01} & \dfrac{1}{Q_1} & jk_{12} & \cdots & jk_{1N} \\ jk_{02} & jk_{12} & \dfrac{1}{Q_2} & \cdots & jk_{2N} \\ \vdots & \vdots & \vdots & \ddots & \vdots \\ jk_{0N} & jk_{1N} & jk_{2N} & \cdots & \dfrac{1}{Q_N} \end{bmatrix}. \tag{33}$$

Referring to Section 2 and to the Appendix A, for the specific analyzed case it is possible to derive:

$$
\begin{aligned}
\tilde{z}_{\text{ii}} &= \frac{2}{Q_0} \\
\mathbf{z}_{\text{io}} &= \begin{bmatrix} jk_{01} & \cdots & jk_{0N} \end{bmatrix} \\
\mathbf{z}_{\text{oi}} &= \mathbf{z}_{\text{io}}^T \\
\tilde{\mathbf{z}}_{\text{oo}} &= \text{diag}\left(\frac{2}{Q_n}\right)
\end{aligned}
\tag{34}
$$

and

$$
\begin{aligned}
c_0 &= \sum_{n=1}^{N} k_{0n}^2 Q_n \\
c_1 &= -c_0 - \frac{2}{Q_0} \\
c_2 &= c_0.
\end{aligned}
\tag{35}
$$

Accordingly, by introducing the parameter α:

$$
\alpha = \sqrt{1 + \sum_{n=1}^{N} k_{0n}^2 Q_0 Q_n},
\tag{36}
$$

for the analyzed case, the solving equation is (see the Appendix A):

$$
(\alpha^2 - 1)\lambda^2 - 2(\alpha^2 + 1)\lambda + (\alpha^2 - 1) = 0.
\tag{37}
$$

Equation (37) has two eigenvalues:

$$
G_{\text{M}} = \frac{\alpha - 1}{\alpha + 1}, \quad G_{\text{M1}} = \frac{\alpha + 1}{\alpha - 1}.
\tag{38}
$$

It is evident that $G_{\text{M1}} > 1$; as a consequence, only G_{M} satisfies the first constrain expressed in (24). By choosing to normalize the input current to 1

$$
i_{\text{iM}} = 1,
\tag{39}
$$

the following normalized eigenvectors can be obtained

$$
i_{\text{oM},n} = -j\frac{k_{0n}Q_n}{\alpha + 1}.
\tag{40}
$$

The corresponding normalized voltages are:

$$
v_{\text{iM}} = \frac{\alpha}{Q_0},
\tag{41}
$$

$$
v_{\text{oM},n} = \frac{1}{\alpha + 1}\left[\left(\sum_{\substack{m=1 \\ m \neq n}}^{N} k_{0m}k_{nm}Q_m\right) + jk_{0n}\alpha\right].
\tag{42}
$$

Hence the optimal normalized source impedance is given by:

$$
z_{\text{GM}} = \frac{v_{\text{iM}}^*}{i_{\text{iM}}^*} = \frac{\alpha}{Q_0},
\tag{43}
$$

however, the optimal N-port load network $\mathfrak{N}_\text{L}$ can be realized as a set of uncoupled loads with normalized impedances:

$$z_{\text{LM},n} = -\frac{v_{\text{oM},n}}{i_{\text{oM},n}} = r_{\text{LM},n} - j\,x_{\text{LM},n} \tag{44}$$

$$r_{\text{LM},n} = \frac{\alpha}{Q_n} \tag{45}$$

$$x_{\text{LM},n} = \frac{1}{k_{0n}Q_n} \sum_{\substack{m=1 \\ m \neq n}}^{N} k_{0m}k_{nm}Q_m \tag{46}$$

The corresponding unnormalized expressions are:

$$R_{\text{LM},n} = \alpha\,R_n \tag{47}$$

$$X_{\text{LM},n} = \frac{R_n}{k_{0n}} \sum_{\substack{m=1 \\ m \neq n}}^{N} k_{0m}k_{nm}Q_m. \tag{48}$$

Discussion of the Results

According to the above reported formulas, the following considerations can be drawn.

- From (38) it is evident that the maximum realizable efficiency of the link only depends on the quality factors of the resonators and on the couplings between the transmitting and the receiving resonators; however, it does not depend on the couplings among the receivers. This means that a possible coupling among the receivers can be always compensated.
- In general, the optimal loads are complex quantities.
- For identical resonators with the same quality factor the real part of the optimal loads is the same for all the loads.
- The imaginary parts of the optimal loads are zero for uncoupled receiving resonators; this means that they play a role of compensation.
- By comparing the expression of the reactive parts of the optimal loads with those of the optimal loads reported in [21] for the maximum power case, it can be easily verified that they are coincident. This means that the same compensating reactances are required for both the maximum efficiency case (i.e., for maximizing the power gain) and the maximum power case.
- The proposed approach also provides the optimal value of the generator impedance, see (27); however, G_p does not depend on the generator. The value provided for Z_G in (27) is that maximizing the power entering the network, and then the power delivered to the loads, when the loads are those maximizing G_p.

It is worth observing that all the achieved results are in a perfect agreement with those reported in [30]. With respect to previously proposed approaches, the theory presented in this paper has the advantage of being completely general, it is valid for any strictly passive and reciprocal network. Additionally, the application of the presented theory just needs the impedance matrix of the link that can be the result of measurements or simulations or theoretical evaluation. In fact, the optimal loads are obtained by solving the eigenvalue problem expressed in (23). To solve the eigenvalue problem one just needs the matrices **A** and **B** that can be directly computed from the **Z** matrix, see (18) and (19).

4. Validation of the Results

To validate the theoretical data, full-wave and circuital simulations have been performed. The commercial tool CST Microwave Studio has been used for full-wave simulations, while the NI AWR Design Environment has been adopted for circuital simulations. Four different WPT links in SIMO configuration have been analyzed. The first three analyzed cases have identical resonators and a different number of receivers, as detailed in the following.

- Case 1: two receivers, see Figure 5a;
- Case 2: three receivers, see Figure 5b;
- Case 3: four receivers, see Figure 5c.

All the analyzed coils (transmitter and receivers) have the same dimensions; they are circular loops with a radius of 5 mm designed by using a copper wire with a radius of 0.3 mm. An operating frequency f_0 of 500 MHz has been assumed. First, the single loop has been analyzed so to calculate the equivalent inductance. From full-wave simulations at f_0 each loop corresponds to an inductance of about 20.9 nH. Accordingly, a series capacitor of 4.84 pF has been added to each loop so to make them resonating at f_0. The relative positions of the transmitting and the receiving coils assumed for the three analyzed cases are illustrated in Figure 5.
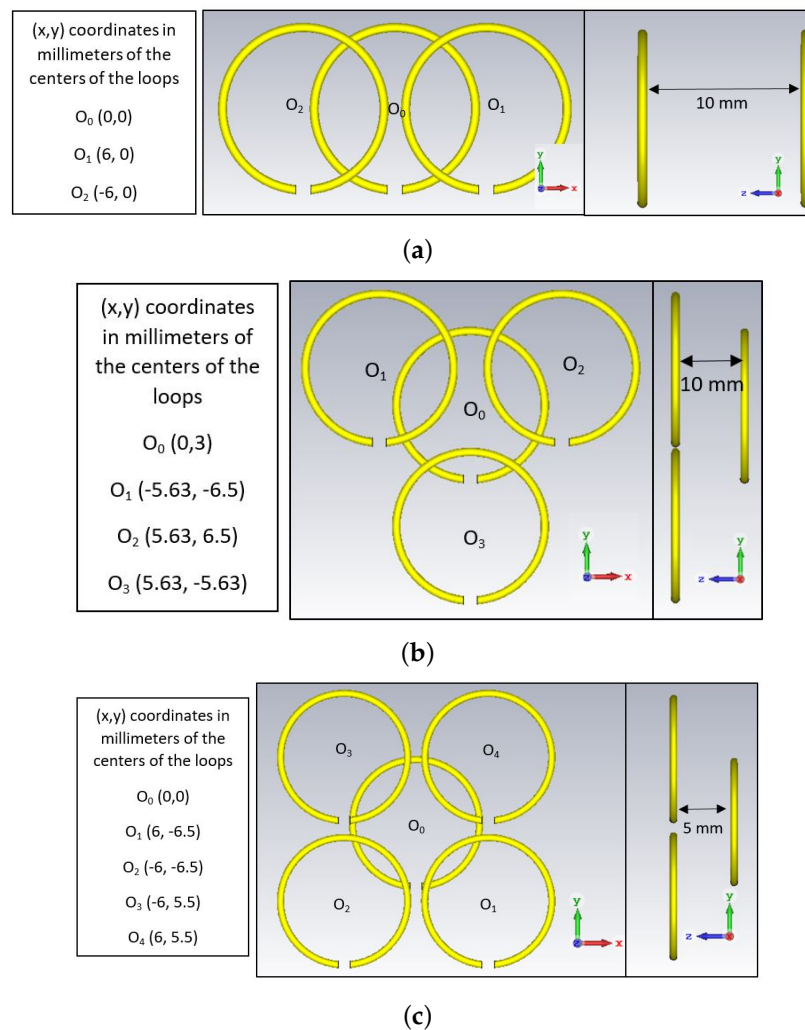
(a)

(b)

(c)

Figure 5. WPT links analyzed through full-wave simulations. (**a**) Case 1: single transmitter and two-receiver link; (**b**) Case 2: single transmitter and three–receiver link; (**c**) Case 3: single transmitter and four-receiver link. In all cases the transmitter is the loop with the center in the point O_0.

To calculate the impedance matrices, each link has been analyzed through full-wave simulations as a multiport network. The following impedance matrices have been obtained:

$$\mathbf{Z_{Case1}} = \begin{pmatrix} 0.118 & 1.41\,j & 1.41\,j \\ 1.41\,j & 0.118 & -2.62\,j \\ 1.41\,j & -2.62\,j & 0.118 \end{pmatrix}, \tag{49}$$

$$\mathbf{Z_{Case2}} = \begin{pmatrix} 0.118 & 2.66\,j & 2.66\,j & 1.17\,j \\ 2.66\,j & 0.118 & -1.84\,j & -1.86\,j \\ 2.66\,j & -1.84\,j & 0.118 & -1.86\,j \\ 1.17\,j & -1.86\,j & -1.86\,j & 0.118 \end{pmatrix}, \tag{50}$$

$$\mathbf{Z_{Case3}} = \begin{pmatrix} 0.118 & 0.81\,j & 0.81\,j & -1.37\,j & -1.37\,j \\ 0.81\,j & 0.118 & -2.60\,j & 0.56\,j & 2.58\,j \\ 0.81\,j & -2.60\,j & 0.118 & 2.58\,j & 0.56\,j \\ -1.37\,j & 0.56\,j & 2.58\,j & 0.118 & -2.60\,j \\ -1.37\,j & 2.58\,j & 0.56\,j & -2.60\,j & 0.118 \end{pmatrix}. \tag{51}$$

By comparing the general expression of the impedance matrix of a resonant inductive WPT link given in (31) with the numerical values calculated through circuital simulations, the values reported in Tables 1–3 have been derived for the coupling coefficients. By using (47) and (48) it is possible to calculate the expressions of the optimal loads. The values calculated for the three analyzed examples are summarized in Tables 1–3. With all the resonators the same quality factor, the resistive part of the loads is the same for all the receivers.

As per the imaginary parts, for the analyzed cases all the calculated values of $X_{\mathrm{LM},n}$ are negative, thus corresponding to load impedances with an inductor $L_{M,n}$ in series configurations with the resistive part $R_{\mathrm{LM},n}$.

Table 1. Parameters of the equivalent circuit and optimal loads of the WPT link illustrated in Figure 5a (Case 1).

$L_n,\ (n=0,1,2)$ (nH)	$C_n,\ (n=0,1,2)$ (pF)	Q	f_0 (MHz)	
20.91	4.84	557	500	
Coupling coefficients				
	k_{01}	k_{02}	k_{12}	
	0.0215	0.0215	−0.0399	
Optimal loads				
α	G_M	R_G (Ω)	$R_{\mathrm{LM},n},\ (n=1,2)$ (Ω)	$L_{\mathrm{LM},n},\ (n=1,2)$ (nH)
16.94	0.89	1.999	1.999	0.835

Table 2. Parameters of the equivalent circuit and optimal loads of the WPT link illustrated in Figure 5b (Case 2).

$L_n,\ (n=0,1,2,3)$ (nH)	$C_n,\ (n=0,1,2,3)$ (pF)		Q		f_0 (MHz)
20.91	4.84		557		500
Coupling coefficients					
k_{01}	k_{02}	k_{03}	k_{12}	k_{13}	k_{23}
0.0406	0.0406	0.0178	−0.0281	−0.0283	−0.0283
Optimal loads					
α	G_M	R_G (Ω)	$R_{\mathrm{LM},n},\ (n=1,2,3)$ (Ω)	$L_{\mathrm{LM},n},\ (n=1,2)$ (nH)	$L_{\mathrm{LM},3}$ (nH)
33.402	0.942	3.941	3.941	0.845	2.695

Table 3. Parameters of the equivalent circuit and optimal loads of the WPT link illustrated in Figure 5c (Case 3).

	L_n, ($n = 0,1,2,3,4$) (nH)	C_n, ($n = 0,1,2,3,4$) (pF)	Q	f_0 (MHz)
	20.91	4.84	557	500

Coupling coefficients									
k_{01}	k_{02}	k_{03}	k_{04}	k_{12}	k_{13}	k_{14}	k_{23}	k_{24}	k_{34}
0.0123	0.0123	-0.0209	-0.0209	-0.0395	0.0084	0.0393	0.0393	0.0084	-0.0395

Optimal loads					
α	G_M	R_G (Ω)	$R_{LM,n}$, ($n = 1,2,3,4$) (Ω)	$L_{LM,n}$, ($n = 1,2$) (nH)	$L_{LM,j}$, ($j = 3,4$) (nH)
19.122	0.901	2.256	2.256	2.522	1.414

The analytical values of the optimal loads have been validated through circuital simulations.

Two different sets of circuital simulations have been performed. A first set of simulations has been performed by modeling the links with lumped elements equivalent circuits with the parameters summarized in Tables 1–3; Figure 6 illustrates the circuit analyzed for case 1. The resistors R_n that appear in Figure 6 are related to the quality factors of the resonators, Q_n, through (29). A second set of simulations has been performed by modeling the analyzed links as $(N + 1)$–port black–box networks described by the impedance matrices provided by full–wave simulations, being N the number of receivers (i.e., $N = 2$ for case 1, $N = 3$ for case 2, $N = 4$ for case 3). In more detail, referring to case 1, simulations have been performed by replacing the network in the dashed square of Figure 6 with a three–port black-box component described by the impedance matrix of the link calculated through circuital simulations.
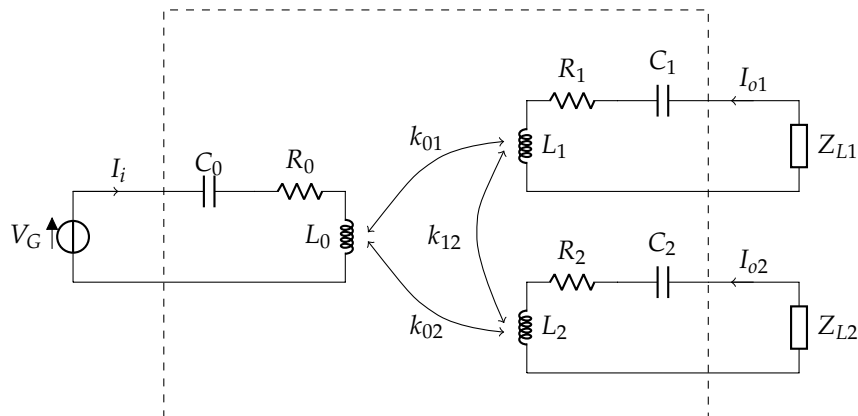

Figure 6. Equivalent circuit analyzed for Case 1.

First, the optimal values provided by the theory for the resistive parts of the loads have been validated. Simulations have been performed by varying the resistive part of the loads, the values calculated for G_P are given in Figure 7a–c.
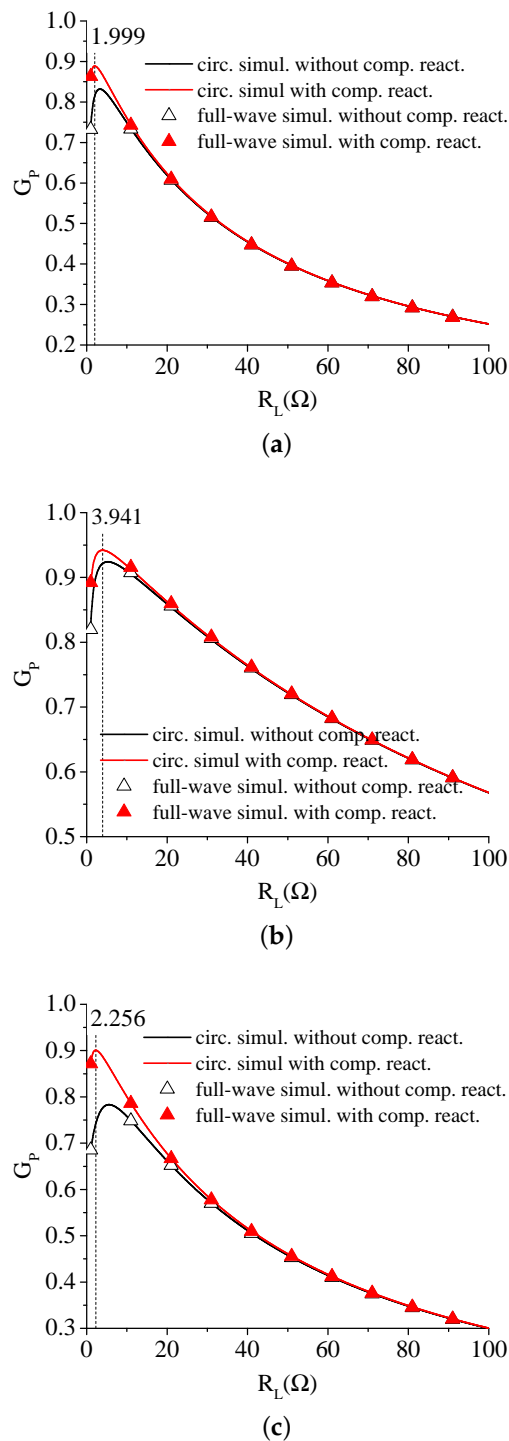
Figure 7. Power gain calculated through circuital simulations by varying the resistive part of the loads R_{Ln}. (**a**) Case 1, the link has two receivers with $R_{L1} = R_{L2} = R_L$; (**b**) Case 2, the link has three receivers with $R_{L1} = R_{L2} = R_{L3} = R_L$; (**c**) case 3, the link has four receivers with $R_{L1} = R_{L2} = R_{L3} = R_{L4} = R_L$. The figure compares full-wave and circuital simulation results obtained for the case of purely resistive loads and for the case of loads with the compensating inductances given in Tables 1–3.

The results obtained for the case of purely resistive loads (i.e., $Z_{Ln} = R_L$) are compared with those obtained for the case of loads with the compensating inductances given in Table 3, i.e., for $Z_{Ln} = R_L + j \omega L_{LM,n}$. In the figures, the triangles have been used for the results obtained by modeling the link with the impedance matrix provided by full-wave simulations; however, the solid

lines have been used for the results obtained by modeling the links with the lumped elements equivalent circuit. It can be seen that the results obtained for the two representations of the links are coincident.

As per the optimal values of R_L, in each figure the value of R_L for which G_P is maximized is highlighted by a dashed vertical line. It can be seen that the values calculated through circuital simulations confirm the theoretical values. Finally, with regard to the compensating inductances $L_{LM,n}$, it seems that they play a more or less important role in maximizing G_P depending on the analyzed case. For instance, according to the achieved results the compensating reactances play a marginal role in maximizing G_P for case 2 while they seem to be more relevant for case 3. However, for all the three analyzed cases it is confirmed that their presence allows obtaining the maximum value of G_P provided by the theory.

The behavior of the power delivered to the loads as function of the generator impedance has been also investigated. Simulations have been performed by using as source a voltage generator with a series impedance R_G. The total output power has been calculated by varying R_G when the loads assume the optimal values provided by the theory. The results are given in Figure 8a–c, data obtained for $Z_{Ln} = R_{LM,n}$ and $Z_{Ln} = R_{LM,n} + j\omega L_{LM,n}$ are compared. The dashed vertical lines highlight the values of R_G maximizing P_o for the case $Z_{Ln} = R_{LM,n} + j\omega L_{LM,n}$. It can be verified that these values are in a perfect agreement with the optimal values provided by the theory. As it can be seen, the use of the generator impedance provided by (43) allows maximizing the power delivered to the loads when they are set to maximize G_P. Additionally, it can be seen that the compensation reactances are crucial to maximize the power transferred to the loads.

It is worth observing that the output power illustrated in Figure 8a–c is the total output power delivered (i.e., the sum of the power delivered to the loads) when the network operates at maximum G_P. From the figures it is evident that if R_G is not optimized, although the network operates with efficiency values close to one, only a small portion of the power available from the generator is delivered to the load.

Finally, the case of a link consisting of three coils with different dimensions has been analyzed (case 4). The geometry analyzed through full-wave simulations is illustrated in Figure 9. All the coils have been designed by using a copper wire with a radius of 0.3 mm. The radius of the transmitting coil is 10 mm, those of the first and second receivers are 7.5 mm and 5 mm, respectively. Also, in this case an operating frequency f_0 of 500 MHz has been assumed.

The impedance matrix as calculated from full-wave simulations is:

$$\mathbf{Z_{Case4}} = \begin{pmatrix} 0.229 & -10.08\,j & 8.66\,j \\ -10.08\,j & 0.145 & 2.82\,j \\ 8.66\,j & 2.82\,j & 0.118 \end{pmatrix}. \tag{52}$$

The parameters derived for the equivalent circuit are summarized in Table 4.

The simulated results obtained for G_P are illustrated in Figure 10. Circuital simulations have been performed by modeling the link as a three–port black–box component described by the impedance matrix calculated through full–wave simulations. In this case, the two receivers have slightly different values of the quality factors; accordingly, the theory predicts slightly different values for $R_{LM,1}$ and $R_{LM,2}$. To verify the expected optimal values, simulations have been performed by terminating the receivers ports on the impedances $Z_{L1} = R_{L1} + j\omega L_{LM,1}$ and $Z_{L2} = R_{L2} + j\omega L_{LM,2}$ and by varying both $R_{L,1}$ and $R_{L,2}$. From Figure 10 it can be seen that circuital simulations confirm the theory, a maximum of about 0.98 is obtained for G_P when $R_{L1} = 11.07\ \Omega$ and $R_{L2} = 9.01\ \Omega$; however, from the figure it can also be seen that values of G_P very close to its maximum (i.e., values greater than 0.97) are obtained for a wide range of values of R_{L1} and R_{L2}.
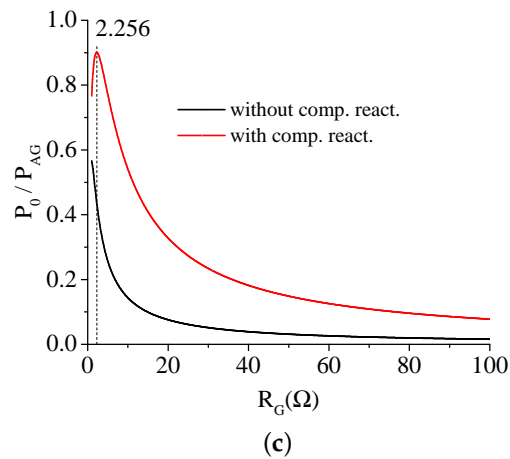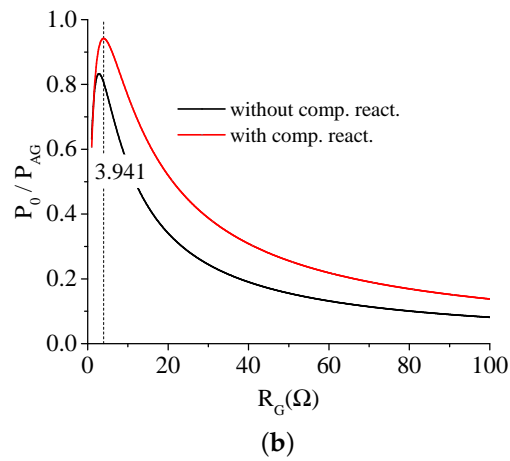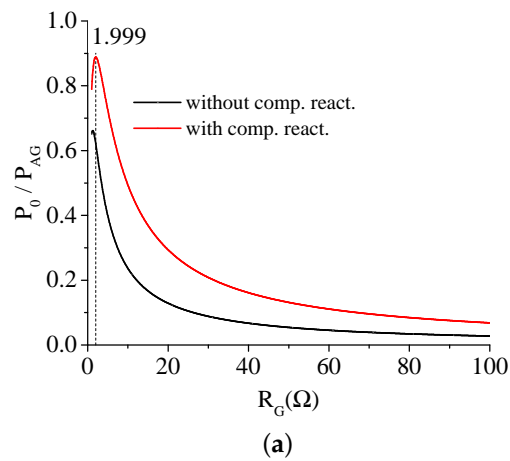
(**a**)

(**b**)

(**c**)

Figure 8. Total output power as function of the generator impedance R_G corresponding to the optimal loads $Z_{LM,n} = R_{LM,n} + j\,X_{LM,n}$; results obtained with and without the compensating reactances $X_{LM,n}$. (**a**) Case 1; (**b**) Case 2; (**c**) Case 3.
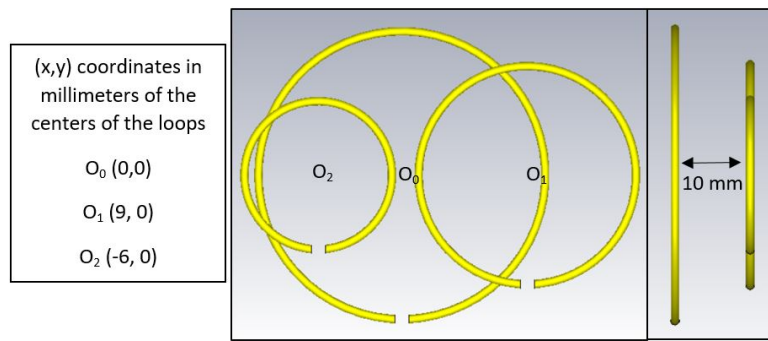
Figure 9. Case 4: WPT link analyzed through full-wave simulations. The link has a single transmitter and two receivers.

Table 4. Parameters of the equivalent circuit and optimal loads of the WPT link illustrated in Figure 9 (Case 4).

L_0 (nH)	L_1 (nH)	L_2 (nH)	C_0 (pF)	C_1 (pF)	C_2 (pF)	Q_0	Q_1	Q_2	f_0 (MHz)
45.38	28.67	20.91	2.23	3.53	4.84	622	621	557	500
Coupling coefficients									
			k_{01}	k_{02}	k_{12}				
			-0.089	0.0894	0.0367				
Optimal loads									
	α	G_M	R_G (Ω)	$R_{LM,1}$ (Ω)	$R_{LM,2}$ (Ω)	$L_{LM,1}$ (nH)	$L_{LM,2}$ (nH)		
	76.38	0.974	17.49	11.07	9.01	0.948	0.852		
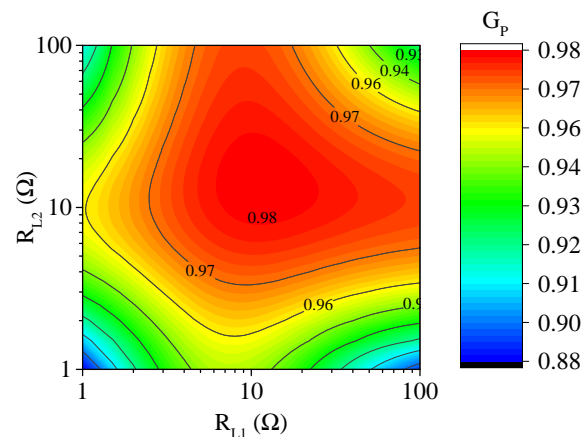
Figure 10. Power gain calculated through circuital simulations for case 4. Results obtained by varying the resistive part of the loads when the reactive parts are set according to the optimal values provided by the theory (see Table 4).

Finally, the behavior obtained for the total output power P_o as function of the generator impedance is illustrated in Figure 11. In this case, simulations have been performed by terminating the ports of the receivers on the optimal load impedances, i.e., $Z_{L1} = R_{LM,1} + j\omega L_{LM,1}$ and $Z_{L2} = R_{LM,2} + j\omega L_{LM,2}$. As for the previously analyzed cases, simulations confirm the importance of suitably selecting the generator impedance for maximizing P_o when the loads are those maximizing G_P.
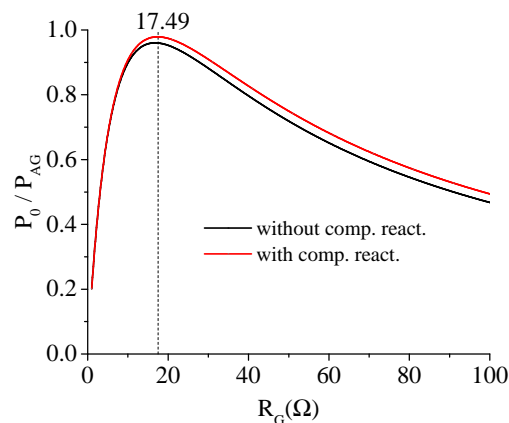
Figure 11. Total output power calculated for case 4 by varying the generator impedance when the loads are those maximizing G_P.

5. Conclusions

In this paper, the case of a WPT link using a Single-Input Multiple-Output (SIMO) configuration is analyzed. The solution for maximizing the efficiency is derived from a generalized eigenvalue problem. The main advantage of the presented theory is its complete generality, no specific assumptions are made about the link. In fact, the proposed approach is valid for any strictly passive and reciprocal $(N + 1)$–port network. Additionally, the desired solution can be derived directly from the impedance matrix with simple algebraic operations. Theoretical formulas for the optimal loads maximizing the efficiency are derived for the case of a resonant inductive link with a generic number N of possibly coupled receivers.

The results obtained this way for the optimal loads are coincident with those reported in the previous literature were the first-order condition on the partial derivatives of the efficiency has been exploited in order to find the desired solution. As a further validation of the derived formulas, several numerical examples have been analyzed through full–wave and circuital simulations. In particular, four different links have been considered. The first three analyzed links use identical resonators for the transmitter and the receivers and differ for the number of receivers. The last analyzed case is a link using two receivers; in this case, the three resonators have been designed so to have different values of the equivalent inductance. More specifically, the transmitter has been designed so to have a larger inductance with respect to the receivers, so to obtain higher values of the couplings with respect to the previously analyzed cases. For all the investigated cases, the impedance matrix has been calculated through full-wave simulations and the presented theory applied so to determine the maximum realizable efficiency and the optimal terminating impedances. The correctness of the analytical data has been verified through simulations performed for evaluating the efficiency of the links. According to the theoretical data, simulations confirm that the maximum realizable efficiency of a resonant inductive link in SIMO configuration does not depend on the coupling among the receiving resonators. In fact, it is demonstrated that a possible coupling among the receivers can be always compensated by using suitable complex loads.

The possibility of maximizing the power delivered to the loads when they are set to maximize the efficiency has been also discussed. In fact, the presented theory provides both:

- the expressions of the loads that maximize the efficiency,
- the expression of the generator impedance that allows maximizing the power entering the network when the loads are those maximizing the efficiency.

Maximizing the power entering the network for a given efficiency corresponds maximizing the power delivered to the loads. The reported results highlight the importance of also optimizing the

generator impedance to avoid that. Despite the high efficiency values, only a small portion of the power available from the generator is transferred to the loads.

As future developments of the presented research, experimental tests will be performed to verify the application of the proposed theory to a real application. Furthermore, in a future work the analysis presented in this paper will be extended to a generic MIMO (Multiple Input Multiple-Output) system.

Appendix A. How to Solve the Generalized Eigenvalue Problem

The following generalized eigenvalue problem is considered:

$$\mathbf{A}\mathbf{x} = \lambda \mathbf{B}\mathbf{x}. \tag{A1}$$

In this Appendix the procedure for calculating the eigenvalues λ and the corresponding eigenvectors $\mathbf{x} = \mathbf{I}$ will be illustrated. By introducing the variable η:

$$\eta = \frac{1}{\lambda} \tag{A2}$$

it is possible to write:

$$\left(\mathbf{B} - \eta \mathbf{A}\right)\mathbf{x} = 0. \tag{A3}$$

By using (18) and (19), it is possible to obtain:

$$\mathbf{B} - \eta \mathbf{A} = \left[\begin{array}{c|c} \tilde{Z}_{\text{ii}} & \mathbf{Z}_{\text{io}} + \eta \mathbf{Z}_{\text{oi}}^{\dagger} \\ \hline \mathbf{Z}_{\text{io}}^{\dagger} + \eta \mathbf{Z}_{\text{oi}} & \eta \tilde{Z}_{\text{oo}} \end{array} \right], \tag{A4}$$

where the following definitions have been introduced:

$$\begin{aligned} \tilde{Z}_{\text{ii}} &= Z_{\text{ii}} + Z_{\text{ii}}^{*} \\ \tilde{Z}_{\text{oo}} &= \mathbf{Z}_{\text{oo}} + \mathbf{Z}_{\text{oo}}^{\dagger}. \end{aligned} \tag{A5}$$

The eigenvalues can be obtained from:

$$\det(\mathbf{B} - \eta \mathbf{A}) = 0. \tag{A6}$$

Considering that for a matrix $\mathbf{M}$ partitioned in 4 submatrix $\mathbf{M}_{11}, \mathbf{M}_{12}, \mathbf{M}_{21}, \mathbf{M}_{22}$:

$$\mathbf{M} = \left[\begin{array}{c|c} \mathbf{M}_{11} & \mathbf{M}_{12} \\ \hline \mathbf{M}_{21} & \mathbf{M}_{22} \end{array} \right], \tag{A7}$$

the determinant is given by:

$$\det(\mathbf{M}) = \det(\mathbf{M}_{11} - \mathbf{M}_{12}\mathbf{M}_{22}^{-1}\mathbf{M}_{21})\det(\mathbf{M}_{22}), \tag{A8}$$

it is possible to write

$$\det(\mathbf{B} - \eta\mathbf{A}) = -\eta^{N-1}(c_0\eta^2 + c_1\eta + c_2)\det(\tilde{\mathbf{Z}}_{\text{oo}}). \tag{A9}$$

where the coefficients c_0, c_1 and c_2 are given by:

$$
\begin{aligned}
c_0 &= \mathbf{Z}_{\text{oi}}^\dagger \tilde{\mathbf{Z}}_{\text{oo}}^{-1}\mathbf{Z}_{\text{oi}}, \\
c_1 &= -\tilde{Z}_{\text{ii}} + \mathbf{Z}_{\text{io}}\tilde{\mathbf{Z}}_{\text{oo}}^{-1}\mathbf{Z}_{\text{oi}} + \mathbf{Z}_{\text{oi}}^\dagger \tilde{\mathbf{Z}}_{\text{oo}}^{-1}\mathbf{Z}_{\text{io}}^\dagger, \\
c_2 &= \mathbf{Z}_{\text{io}}\tilde{\mathbf{Z}}_{\text{oo}}^{-1}\mathbf{Z}_{\text{oi}}^\dagger.
\end{aligned}
\tag{A10}
$$

Accordingly, the non-trivial solutions are provided by the equation:

$$c_2\lambda^2 + c_1\lambda + c_0 = 0. \tag{A11}$$

References

1. Karalis, A.; Joannopoulos, J.D.; Soljačić, M. Efficient wireless non-radiative mid-range energy transfer. *Ann. Phys.* **2008**, *323*, 34–48. [CrossRef]
2. Monti, G.; Paolis, M.V.D.; Corchia, L.; Tarricone, L. Wireless Resonant Energy link for Pulse Generators Implanted in the Chest. *IET Microw. Antennas Propag.* **2017**, *11*, 2201–2210. [CrossRef]
3. Carvalho, N.B.; Georgiadis, A.; Costanzo, A.; Stevens, N.; Kracek, J.; Pessoa, L.; Rogier, H. Europe and the future for WPT. *IEEE Microw. Mag.* **2017**, *18*, 56–87. [CrossRef]
4. Rim, C.T.; Mi, C. *Wireless Power Transfer for Electric Vehicles and Mobile Devices*; Wiley-IEEE Press: Hoboken, NJ, USA, 2017.
5. Inagaki, N. Theory of Image Impedance Matching for Inductively Coupled Power Transfer Systems. *IEEE Trans. Microw. Theory Tech.* **2014**, *62*, 901–908. [CrossRef]
6. Mastri, F.; Mongiardo, M.; Monti, G.; Dionigi, M.; Tarricone, L. Gain expressions for resonant inductive wireless power transfer links with one relay element. *Wirel. Power Transf.* **2018**, *5*, 27–41. [CrossRef]
7. Monti, G.; Costanzo, A.; Mastri, F.; Mongiardo, M. Optimal design of a wireless power transfer link using parallel and series resonators. *Wirel. Power Transf.* **2016**, *3*, 105–116. [CrossRef]
8. Yoon, I.; Ling, H. Investigation of near-field wireless power transfer under multiple transmitters. *IEEE Antenna Wirel. Propag. Lett.* **2011**, *10*, 662–665. [CrossRef]
9. Pacini, A.; Costanzo, A.; Aldhaher, S.; Mitcheson, P.D. Load- and Position-Independent Moving MHz WPT System Based on GaN-Distributed Current Sources. *IEEE Trans. Microw. Theory Tech.* **2017**, *65*, 5367–5376. [CrossRef]
10. Lang, H.D.; Ludwig, A.; Sarris, C.D. Convex Optimization of Wireless Power Transfer Systems with Multiple Transmitters. *IEEE Trans. Antennas Propag.* **2014**, *62*, 4623–4636. [CrossRef]
11. Monti, G.; Che, W.; Wang, Q.; Costanzo, A.; Dionigi, M.; Mastri, F.; Mongiardo, M.; Perfetti, R.; Tarricone, L.; Chang, Y. Wireless Power Transfer with Three-Ports Networks: Optimal Analytical Solutions. *IEEE Trans. Circuits Syst.* **2017**, *62*, 494–503. [CrossRef]
12. Arakawa, T.; Goguri, S.; Krogmeier, J.V.; Kruger, A.; Love, D.J.; Mudumbai, R.; Swabey, M.A. Optimizing wireless power transfer from multiple transmit coils. *IEEE Access* **2018**, *6*, 23828–23838. [CrossRef]
13. Kim, G.; Boo, S.; Kim, S.; Lee, B. Control of Power Distribution for Multiple Receivers in SIMO Wireless Power Transfer System. *J. Electromagn. Eng. Sci.* **2018**, *18*, 221–230. [CrossRef]
14. Cai, W.; Ma, D.; Tang, H.; Lai, X.; Liu, X.; Sun, L. Highly Efficient Target Power Control for Two-Receiver Wireless Power Transfer Systems. *Energies* **2018**, *11*, 2726. [CrossRef]
15. Liu, M.; Fu, M.; Wang, Y.; Ma, C. Battery Cell Equalization via Megahertz Multiple-Receiver Wireless Power Transfer. *IEEE Trans. Power Electron.* **2018**, *33*, 4135–4144. [CrossRef]
16. Cai, W.; Lai, X.; Ma, D.; Tang, H.; Hashmi, K.; Xu, J. Management of Multiple-Transmitter Multiple-Receiver Wireless Power Transfer Systems Using Improved Current Distribution Control Strategy. *Electronics* **2019**, *8*, 1160. [CrossRef]
17. Luo, C.; Qiu, D.; Lin, M.; Zhang, B. Circuit Model and Analysis of Multi-Load Wireless Power Transfer System Based on Parity-Time Symmetry. *Energies* **2020**, *13*, 3260. [CrossRef]

18. Wagih, M.; Komolafe, A.; Zaghari, B. Dual-Receiver Wearable 6.78 MHz Resonant Inductive Wireless Power Transfer Glove Using Embroidered Textile Coils. *IEEE Access* **2020**, *8*, 24630–24642. [CrossRef]

19. Ahn, D.; Kim, S.; Kim, S.; Moon, J.; Cho, I. Wireless Power Transfer Receiver with Adjustable Coil Output Voltage for Multiple Receivers Application. *IEEE Trans. Ind. Electron.* **2019**, *66*, 4003–4012. [CrossRef]

20. Vu, V.; Phan, V.; Dahidah, M.; Pickert, V. Multiple Output Inductive Charger for Electric Vehicles. *IEEE Trans. Power Electron.* **2019**, *34*, 7350–7368. [CrossRef]

21. Monti, G.; Dionigi, M.; Mongiardo, M.; Perfetti, R. Optimal Design of Wireless Energy Transfer to Multiple Receivers: Power Maximization. *IEEE Trans. Microw. Theory Tech.* **2017**, *65*, 260–269. [CrossRef]

22. Fu, M.; Yin, H.; Liu, M.; Wang, Y.; Ma, C. A 6.78 MHz Multiple-Receiver Wireless Power Transfer System with Constant Output Voltage and Optimum Efficiency. *IEEE Trans. Power Electron.* **2018**, *33*, 5330–5340. [CrossRef]

23. Lin, H.; Li, L. Efficiency Analysis and Optimization for Multiple-Receiver Magnetic Coupling Resonant Wireless Power Transfer System. In Proceedings of the 2020 5th International Conference on Computer and Communication Systems (ICCCS), Shanghai, China, 22–24 February 2020; pp. 742–747.

24. Lee, K.; Chae, S.H. Comparative Analysis of Frequency-Selective Wireless Power Transfer for Multiple-Rx Systems. *IEEE Trans. Power Electron.* **2020**, *35*, 5122–5131. [CrossRef]

25. Fu, M.; Zhang, T.; Ma, C.; Zhu, X. Efficiency and Optimal Loads Analysis for Multiple-Receiver Wireless Power Transfer Systems. *IEEE Trans. Microw. Theory Tech.* **2015**, *63*, 3463–3477. [CrossRef]

26. Fu, M.; Zhang, T.; Zhu, X.; Luk, P.C.; Ma, C. Compensation of Cross Coupling in Multiple-Receiver Wireless Power Transfer Systems. *IEEE Trans. Ind. Inform.* **2016**, *12*, 474–482. [CrossRef]

27. Ishihara, M.; Fujiki, K.; Umetani, K.; Hiraki, E. Automatic Active Compensation Method of Cross-Coupling in Multiple-receiver Resonant Inductive Coupling Wireless Power Transfer Systems. In Proceedings of the 2019 IEEE Energy Conversion Congress and Exposition (ECCE), Baltimore, MD, USA, 29 September–3 October 2019; pp. 4584–4591.

28. Duong, Q.T.; Okada, M. Maximum efficiency formulation for inductive power transfer with multiple receivers. *IEICE Electron. Exp.* **2016**, *22*, 20160915. [CrossRef]

29. Yuan, Q.; Aoki, T. Practical applications of universal approach for calculating maximum transfer efficiency of MIMO-WPT system. *Wirel. Power Transf.* **2020**, *7*, 86–94. [CrossRef]

30. Duong, Q.; Okada, M. Maximum Efficiency Formulation for Multiple-Input Multiple-Output Inductive Power Transfer Systems. *IEEE Trans. Microw. Theory Tech.* **2018**, *66*, 3463–3477. [CrossRef]

31. Desoer, C. The maximum power transfer theorem for n-ports. *IEEE Trans. Circuit Theory* **1973**, *20*, 328–330. [CrossRef]